Published in "Physical Review A 78:032701,2008"
which should be cited to refer to this work.

Absolute cross sections for dissociative electron attachment to HCl, HBr, and their deuterated analogs

J. Fedor, O. May, and M. Allan
Department of Chemistry, University of Fribourg, Chemin du Musée 9, 1700 Fribourg, Switzerland

We have measured absolute dissociative electron attachment cross sections for HX and DX (X=Cl and Br) using a trochoidal electron spectrometer equipped with a total ion collection collision chamber, operated both in a field-free passive ion collection mode, and an active ion collection mode, with an extracting electric field. Our results for Br^- from HBr are in an excellent quantitative agreement with recent predictions of the nonlocal resonance model, but the cross sections for Cl^- from HCl and DCl are, respectively, 2.2 times and 2.8 times smaller than the theoretical predictions. Cross sections for the production of H^- and D^- in the 6–10 eV range are much smaller than those for X^- and the isotope effect is much weaker, consistent with the assignment to core-excited Feshbach resonances. There is one exception, however, the 9 eV band in HCl has a large isotope effect.

PACS number(s): 34.80.Ht, 52.20.Fs

I. INTRODUCTION

Hydrogen halides represent a particularly attractive class of compounds for the study of electron-molecule collisions, because of a number of interesting phenomena encountered in the cross sections [1]. These resonance phenomena are much more complex than simple shape resonances, and their description requires the use of theory extending beyond the local complex potential model. At the same time these molecules are small enough to be treated by such high level theories. The cross sections are also of practical importance because hydrogen halides are used in industrial plasmas [2,3].

The interesting phenomena include threshold peaks in vibrational excitation (VE) cross sections [4], Wigner cusps, structures due to vibrational Feshbach resonances (VFR) and outer well resonances in the elastic and VE cross sections [5,6], steps due to interchannel coupling in dissociative electron attachment (DEA) [7,8] and associative electron detachment (AED) [9,10], and dramatic dependence of the DEA cross section on initial vibrational and rotational excitation of the target [11,12]. Many of these phenomena are related to the capacity of these molecules to weakly bind an electron by dipole and polarizability attraction at extended internuclear distances (in the fixed nuclei picture). Several methods of theoretical treatment of this problem were developed, most relevant to the present work being the nonlocal resonance theory [13] which has so far succeeded in reproducing all of the subtleties of the available experimental observations [5,14,15]. A more exhaustive list of references to both the experimental and the theoretical work has been given in the review paper of Hotop *et al.* [1], and, even more recently, by Fedor *et al.* [11].

The nonlocal resonance theory is very versatile in the sense that one and the same model is capable of describing the entire range of phenomena listed above, including the magnitudes of the cross sections. It is thus desirable to test all of its predictions, that is all final channels (elastic, VE, DEA), wide ranges of rotational and vibrational states of the target, and to test both the qualitative aspects, the intricate structures in the cross sections, and the quantitative aspects, the absolute values of the cross sections. Not all the required experimental data has been measured, however, and the present work aims at closing one such gap by measuring the absolute magnitudes of the DEA cross sections.

Only few measurements of absolute DEA cross sections have been reported so far for hydrogen halides. An early measurement of HCl and HBr was reported by Buchelnikova [16]. There are two measurements of the Cl^-/DCl and Cl^-/HCl cross section. That of Christophorou *et al.* [17] is based on a beam experiment combined with an attachment rate measurement in a swarm, the other, by Azria *et al.* [18], used a total ion collection experiment, normalized by measurement of the positive ion current and the known ionization cross section. The results of the three measurements differ dramatically, however. Christophorou *et al.* also measured Br^-/HBr and Br^-/DBr cross sections, but since their result for HCl, in particular the HCl/DCl isotope effect, was very different from that of Azria *et al.* [18], the reliability of these data is questionable, Orient and Srivastava [19] measured the HCl cross sections using a crossed beam, relative flow method. Absolute theoretical cross sections relevant to this work were given by Teillet-Billy and Gauyacq [20], Fabrikant *et al.* [21] and Horáček *et al.* [14].

DEA to HBr/DBr and HCl/DCl has also been reported at higher electron energies (6 to 10 eV), leading to H^- and D^- ions. The corresponding cross sections have been measured for HCl and DCl by Azria *et al.* [18] and for HCl by Orient and Srivastava [19]. To our knowledge, there are no absolute cross-section measurements for H^- and D^- channels for HBr and DBr.

The importance of the absolute DEA cross sections is increased by the fact that DEA data is complementary to that for the reverse process AED, and the same theoretical model was used to describe both. Both absolute cross section [22] and various structures in spectra resolved with respect to the populations of the final states [9,10] have been measured for AED. AED is nominally the reverse process of DEA, but in reality the experiments are complementary because they probe different ranges of rotational and vibrational states of

the molecule. DEA experiments probe molecular states with low rotational (J) and vibrational (v) quanta, given by their initial thermal population, whereas AED probes high J's, given by the distribution of the impact parameters in the X^-+H collisions, and high v's, which are preferentially populated in this process. The gap between the two regimes is partially bridged by DEA experiments on hot targets, where higher J's and v's are excited thermally [11,12].

The present paper focuses on the yield of Br^- and Cl^- fragments, which are produced at electron energies below 1.5 eV and for which the nonlocal resonance model is applicable, but for completeness we shall also present the cross sections for H^- yield in the 6–10 eV range. The experimental setup will be described in some detail.

II. EXPERIMENT

The methods which are currently used by other research groups to measure absolute DEA cross sections are the total ion collection principle (e.g., Refs. [23,24]), the relative flow method (e.g., Ref. [25]) or the combination of the swarm and the beam data (e.g., Ref. [26]).

We have modified an existing trochoidal electron spectrometer [27] to incorporate a total ion collection tube. The cross section σ is determined as

$$\sigma = \frac{I_i}{I_e n_g l}, \tag{1}$$

where I_i is the current of created ions, n_g is the number density of the gas, I_e is the current of passing electrons, and l is the length of the interaction path. A critical point in the cross-section determination is the reliable measurement of the ion current. We have adopted the approach of measuring I_i in the total ion collection mode without mass selection. It is an old technique [28] but has been thoroughly tested and proved [29].

Only the crucial part of the new instrument, the collision chamber with ion collection, is presented here in detail, the remainder was described previously [10,27]. The collision chamber is shown schematically in Fig. 1. The electron beam, confined by an axial magnetic field, enters and exits the interaction region through two orifices with a diameter of 1 mm. The electron path is surrounded by six ion collectors, molybdenum sheets 2 cm (inner ones) and 1 cm (outer ones) long. The design of the chamber is based on charged particle trajectory calculations [30].

Use is made of the fact that ions have much larger gyroradii than electrons, are not confined by the magnetic field, and arrive at the collectors. The feedthroughs leading to the collectors are electrically guarded, the current is transported to an electrometer by shielded semirigid coaxial cables. The chamber was operated in two modes that differ in the way in which the ions are collected: (i) passive collection mode with a field-free chamber and (ii) active collection mode where ions are extracted with an electric field.

The passive collection mode, is similar to that used by Burrow and co-workers [29]. All six sheets are grounded, the chamber is field-free, and the collection of the ions relies on their initial kinetic energies. In the present case the kinetic

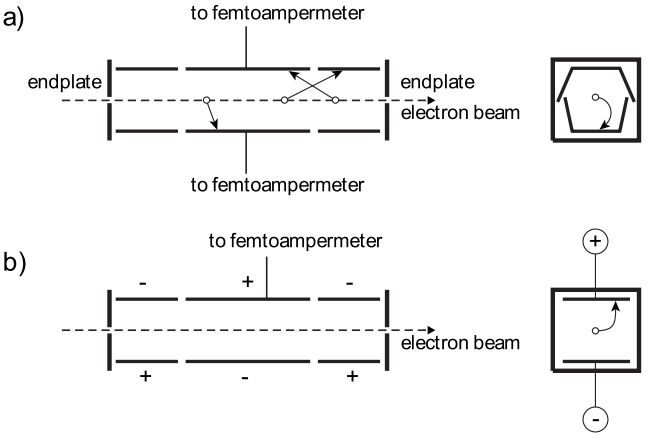

FIG. 1. Schematic view of the collision chamber (a) in the passive collection mode and (b) in the active collection mode. The left-hand side shows the arrangements of the voltages on the molybdenum sheets, on the right-hand side are the cross sections of the chamber.

energy release is very small because the Br^- and Cl^- ions are formed very close to threshold and because most of the excess energy is retained by the lighter fragment, H or D. Initial thermal kinetic energy assists collection in this case. We measured the ion current only on the two inner electrodes (l=2 cm), to compensate for the end effect, the loss of ions that are not collected on the inner sheets due to the longitudinal component of their initial kinetic energy, as shown in Fig. 1. A small fraction of the ions with nearly axial velocities will hit the end plates and not be compensated, however. The fraction of ions lost in this way depends on the angular distribution.

In the active collection mode, a symmetric extraction voltage is applied across the inner sheets and the ion current is measured on the positive sheet. This mode is similar to that used by Rapp, Briglia, and co-workers [28,31,32]. The strength of the extraction field is adjusted for each particular fragment until the ion current reaches saturation and this mode thus does not suffer from the loss of ions on the end plates. It has two other problems, however.

The ion extraction field deflects the primary electron beam sideways from its axial path due to the trochoidal $E \times B$ drift, particularly at low incident energies. This problem is overcome by applying voltages of opposite polarities to the outer sheets, causing the beam to drift in an opposite direction here. Because the combined length of the outer sheets is the same as the length of the inner sheets, the drifts compensate and the electrons arrive at the exit orifice. This scheme is useful down to an energy of 50 meV for the extraction fields of 4 V/cm to 6 V/cm used in the present measurements.

The second problem is a large background caused by electrons scattered inelastically such as to lose nearly all of their energy. These slow electrons drift sideways and reach the sides of the U-shaped electrodes shown in Fig. 1(a). Large amounts of nearly zero eV electrons are produced at the energies of shape resonances in polyatomic molecules [27] and interfere, for example, with the O^-/CO_2 measurement which we used for verification. This problem is avoided by replac-

ing the U-shaped collectors by flat sheets as shown in Fig. 1(b) before measuring in the active collection mode, with the inconvenience of having to open the vacuum system each time when the ion collection mode was changed.

A general problem of the total ion collection tube is a background current due to the multiply elastically or inelastically scattered electrons, which change their direction at the collisions and thus by-pass the collimating effect of the magnetic field and arrive at the ion collectors. In order to minimize this effect, we operate the spectrometer with a rather high magnetic field of approximately 320 G. We also found that this background rises with pressure faster than linearly, and its magnitude relative to signal improves when working at low sample gas pressures. The strong magnetic field decreases, unfortunately, the electron energy resolution of the trochoidal monochromator because of smaller Larmor radii and therefore reduced rejection of electrons with perpendicular momentum [33]. The resolution during the present measurements was of the order of 200 meV.

The original trochoidal electron analyzer [10,27] was still mounted at the exit of the new target chamber, but all its electrodes were short-circuited, kept at +25 V, and functioned as a Faraday cup which measured the electron beam current behind the collision chamber. Burrow and co-workers [34] reported that electrons which are reflected, instead of collected, at the Faraday cup can reenter the target chamber, increase the effective beam current, and falsify the measurements. We have the possibility to prevent the reflection in the same way as used by Burrow and co-workers, by applying a voltage across the deflectors of the original trochoidal analyzer, but we have not seen any influence of the deflectors' voltage on the measured cross section. It seems that the complex setup of the double trochoidal analyzer prevents electron reflection even without a perpendicular electric field.

The collision chamber has two 1/4 inch outer diameter tubes connected to it, one serves as the gas inlet, the second one leads to a capacitance pressure gauge. The typical sample pressure during the present measurements was 1×10^{-4} Torr. At this pressure, the attenuation of the electron beam current due to electron scattering on the sample gas is below 3%.

The problems encountered with the ion collection are different for the two modes of ion collection and using both for each measurement represents an important consistency check. We consider the difference in the resulting cross sections, which is typically better than $\pm 15\%$, to be an indication of the error related to ion collection. We further confirmed the reliability of the apparatus by repeatedly measuring the cross sections for O^-/O_2, O^-/CO_2, and O^-/N_2O, and obtained good agreement with the results of Rapp and Briglia [31]. Representative values were given in our earlier presentation [35]. We estimate our cross sections to be reliable within $\pm 20\%$.

A residual gas analyzer was attached to the vacuum chamber and used to monitor the isotopic purity of the sample.

III. RESULTS AND DISCUSSION

A. Cl^- and Br^- fragments

Figure 2 shows the cross sections for the heavy fragments Cl^- and Br^- in the two measurement modes. The dotted lines

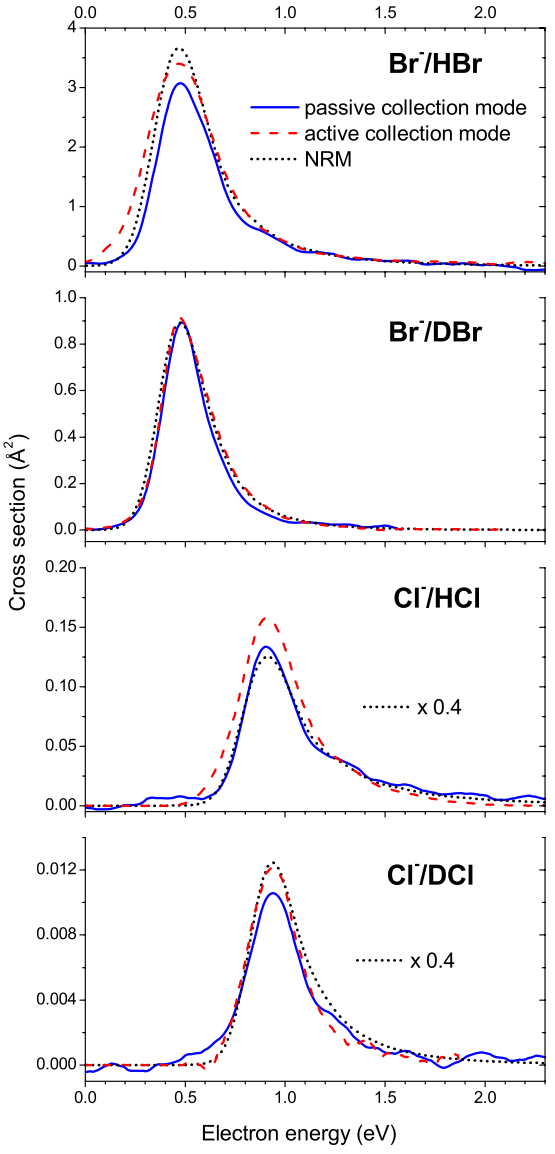

FIG. 2. (Color online) DEA cross sections. Full lines, measured in the passive collection mode; dashed lines, with active ion extraction. The dotted lines are results of the nonlocal resonance model [14] convoluted with a 200 meV FWHM Gaussian electron energy resolution. They were multiplied by a factor of 0.4 in the HCl and DCl case.

show the predictions of the nonlocal resonant model (NRM) [14] convoluted with a Gaussian electron energy resolution function with 200 meV full width at half-maximum (FWHM). For the HCl and DCl case the theoretical cross sections exceeded the experimental values considerably and they were multiplied by a factor of 0.4 for the sake of comparison. Since the inherent fragment ion peaks are rather narrow, their widths in the spectra and the peak values of the cross sections depend on the experimental electron energy resolution. A more suitable quantity for comparison between theory and experiment is therefore the energy-integrated cross section

TABLE I. Energy integrated cross sections σ_I (in units of Å^2 eV), and isotope ratios.

Ion	This work	NRM [14]	Previous experimental work		Other theoretical work
Br^-/DBr	0.30	0.32	0.51 [17]		
Br^-/HBr	1.36	1.54	0.74 [17]	0.20 [16]	
Cl^-/DCl	0.45×10^{-2}	1.25×10^{-2}	6.0×10^{-2} [17]	0.704×10^{-2} [18]	0.234×10^{-2} [20]
Cl^-/HCl	6.85×10^{-2}	14.9×10^{-2}	7.4×10^{-2} [17]	3.52×10^{-2} [18]	3.32×10^{-2} [20]
			13.7×10^{-2} [19]	1.5×10^{-2} [16]	15.0×10^{-2} [21]
$\sigma_I(HBr)/\sigma_I(DBr)$	4.53	4.81	1.45 [17]		
$\sigma_I(HCl)/\sigma_I(DCl)$	15.3	11.9	1.23 [17]	5.0 [18]	14.2 [20]

$$\sigma_I = \int_{\epsilon=0}^{\infty} \sigma(\epsilon) d\epsilon, \tag{2}$$

where ϵ is the electron energy, and which is listed in Table I.

The present Cl^-/HCl cross section agrees well with that of Christophorou *et al.* [17], but there is a dramatic disagreement about the isotope effect, 1.2 in their work and 15.3 in the present work. We found that several days of passivation are required when switching from HCl to DCl before all hydrogens in the inlet system are exchanged and a high isotopic purity is reached. A possible explanation of the dramatically overestimated DCl cross section could thus be an insufficient passivation. The isotope effect for HBr is also much smaller in the work of Christophorou *et al.* than in the present measurement. The HCl cross section of Azria *et al.* [18] is about 2 times smaller than the present value. Their isotope effect, 5.0, is larger than that of Christophorou *et al.*, but still much smaller than the present value. The results of Buchelnikova [16] are about 5 times too small for both HCl and HBr.

The present results for HBr are in excellent agreement with the predictions of nonlocal resonance theory of Horáček *et al.* [14], both in terms of absolute values and of the isotope effect. Relative cross sections for HBr and DBr were already measured in our laboratory at high resolution (10 meV) [15] using an electrostatic electron spectrometer [36]. The present data permits to convert the relative spectra to absolute cross sections, by renormalizing them to obtain the correct energy-integrated cross section measured in this work. The results, permitting an ultimate comparison of theory and experiment, are shown in Fig. 3. The overall agreement is excellent, with the only difference being that the experimental cross sections are slightly lower at higher energies. The agreement is also very good for the hot bands, due to DEA to thermally rotationally and vibrationally (in the case of DBr) excited target molecules. Note that, although the energy-integrated cross section for HBr is 4.5 times larger than the DBr cross section, the peak value is only about 2 times larger. The smaller energy-integrated cross section in DBr is partly a consequence of the fact that the $v=2$ threshold, and the DEA drop associated with it through interchannel coupling, are only slightly above the DEA threshold, making the Br^-/DBr peak narrower than the Br^-/HBr peak.

The predictions of the nonlocal resonance model for HCl and DCl agree less well with the experiment, they are 2.2 and 2.8 times larger than the experimental values, respectively (Fig. 2 and Table I). In judging the difference it should be born in mind, however, that the absolute value of the cross section is a steep exponential function of some parameters of the model, in particular the resonance width, and small changes of these parameters cause large changes of the cross sections. The theory overestimates the cross sections and underestimates the isotope effect. Since, for DEA mediated by a resonance with a large autodetachment width Γ, the DEA cross section decreases and the isotope effect increases with increasing Γ, our observations are qualitatively consistent with the conclusion that the effective Γ of the model for HCl should be increased. Our conclusion is thus that the present

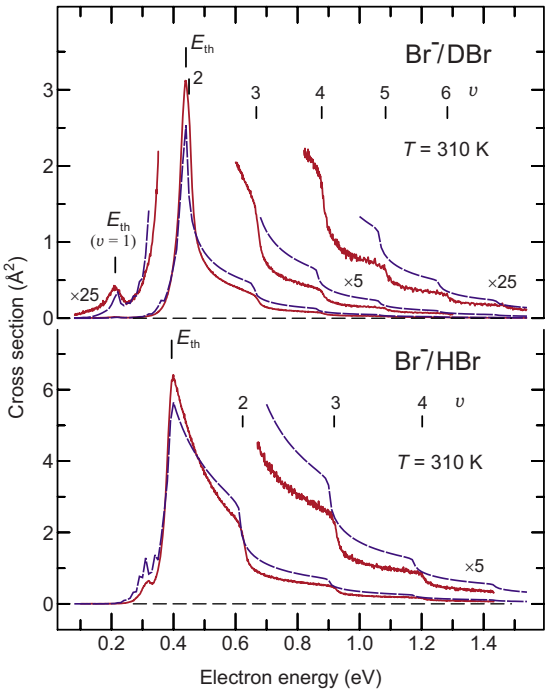

FIG. 3. (Color online) Solid lines: high resolution (10 meV) absolute cross sections for Br^-/HBr and Br^-/DBr, obtained by normalizing earlier relative spectra [15] to the present absolute values. Dashed lines: predictions of the nonlocal resonance theory [14,15], with the final temperature taken into account, but without convolution with an apparatus function. Note that the experimental and theoretical data sets are independently on absolute scales, without any mutual normalization or scaling. The vibrational thresholds (v) and the DEA thresholds E_{th} are indicated.

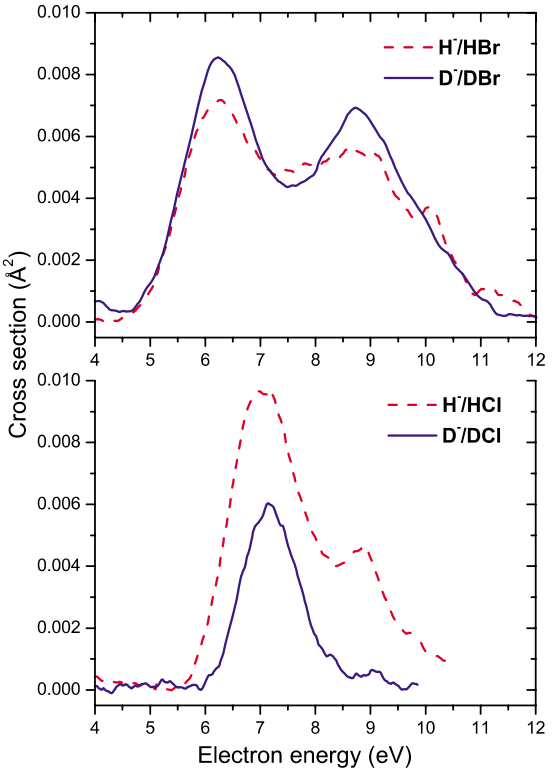

FIG. 4. (Color online) Cross sections for production of H^- and D^-.

disagreement with theory does not indicate any surprising physics, the nonlocal resonance theory is fundamentally correct, and agreement can be reached by adjusting the parameters of the model for HCl. Since $\Gamma(R,E)$ is a function of the internuclear distance R and the energy E in the NRM, there is no simple way to decide in which way it should be changed, however.

We note that in the NRM, the negative ion potential function consists of a short-range part, obtained from fitting the *ab initio* electron-molecule scattering data and the long-range part, obtained from fitting the *ab initio* data on the bound negative ion. The NRM for HBr has been constructed by Čížek *et al.* [15] using the electron-scattering *ab initio* data of Fandreyer *et al.* [37]. The model for HCl has been constructed by Čížek *et al.* [38], using the short-range part of Domcke and Mündel [39], who fitted the *ab initio* electron-scattering data of Padial and Norcoss [40], which is substantially older than the data of Fandreyer *et al.* [37] for HBr. We thus suggest that it may be helpful to repeat the electron-scattering calculation for HCl and fit the NRM to the new results.

The predictions of the effective range calculation of Teillet-Billy and Gauyacq for HCl and DCl [20] are too low by nearly a factor of 2, but their isotope effect is correct. The calculated HCl cross section of Fabrikant *et al.* [21] is larger than the present measurement.

B. H^- and D^- fragments

The cross sections for the H^- and D^- fragments are shown in Fig. 4 and the peak cross sections are listed in Table II. The average of the cross sections from the two measurement modes is shown in the figure and given in the table. A smoothly varying weak background must be subtracted from the spectra in this energy region. This background was growing with electron energy and we suppose that it was due to multiply elastically scattered electrons.

Our cross sections are nearly 2 times larger than those of Azria *et al.* [18]. This is about the same ratio as for the Cl^- cross sections, that is, the ratio of the Cl^- and H^- cross sections is about the same in both studies. This is an important verification of consistency in view of the very different kinetic energy releases for the Cl^- and H^- fragments. Also the isotope effect is about the same in both measurements. Our cross sections are nearly 2 times smaller than those of Orient and Srivastava [19].

The isotope effect for the production of light fragments is much smaller than that for the production of heavy fragments. The cross section for D^-/DBr even appears to be larger than that for H^-/HBr, but the difference lies within the experimental error. The angular distribution measurements of Le Coat *et al.* [41] for H^-/HBr and of Azria *et al.* [42] for H^-/HCl indicated that in both molecules the first peak can be attributed to a $^2\Sigma$, the second peak to a $^2\Pi$ resonance. We conclude that all the resonant states involved have small autodetachment widths, except the $^2\Pi$ resonance responsible for the second peak in HCl, where a large isotope effect is observed.

IV. CONCLUSIONS

The present absolute experimental cross sections for dissociative electron attachment yielding Br^- from HBr and DBr are both in excellent agreement with the predictions of the nonlocal resonance theory of Horáček *et al.* [14]. The combination of the present absolute values with earlier highly resolved but relative spectra [15] yields data which is

TABLE II. Peak cross sections for H^- and D^- production in the 5–11 eV range, in units of Å^2.

	This work		Reference [18]		Reference [19]	
Ion	First band	Second band	First band	Second band	First band	Second band
D^-/DBr	8.5×10^{-3}	6.9×10^{-3}				
H^-/HBr	7.2×10^{-3}	5.6×10^{-3}				
D^-/DCl	6.0×10^{-3}	0.06×10^{-3}	2.9×10^{-3}	$\leqslant 2.1\times10^{-3}$		
H^-/HCl	9.6×10^{-3}	4.6×10^{-3}	5.2×10^{-3}	2.8×10^{-3}	20.7×10^{-3}	9.3×10^{-3}

both absolute and highly resolved. The resulting spectra agree with the theoretical predictions in all details.

The predictions of the nonlocal resonance model for HCl and DCl are, respectively, 2.2 times and 2.8 times larger than the present experimental results. The calculation thus overestimates the values of the cross sections and underestimates the isotope effect, indicating that the model used in the calculation underestimates the autodetachment width. We recommend that a new scattering calculation is performed for HCl on which the nonlocal resonance model could be fitted.

The cross sections for H^- and D^- production in the 6–12 eV range were measured to be much smaller and with a generally small isotope effect, consistent with an assignment to Feshbach resonances. An exception is the isotope effect of the 9 eV resonance in HCl which is, surprisingly, much larger.

ACKNOWLEDGMENTS

We thank J. Horáček and M. Čížek for valuable comments. This research is part of Contract No. 200020-113599/1 of the Swiss National Science Foundation and of COST Action CM0601.

[1] H. Hotop, M.-W. Ruf, M. Allan, and I. I. Fabrikant, Adv. At., Mol., Opt. Phys. **49**, 85 (2003).
[2] O. Šašić, S. Dujko, Z. L. Petrović, and T. Makabe, Jpn. J. Appl. Phys., Part 1 **46**, 3560 (2007).
[3] O. Šašić and Z. L. Petrović, Radiat. Phys. Chem. **76**, 573 (2007).
[4] K. Rohr and F. Linder, J. Phys. B **8**, L200 (1975).
[5] M. Allan, M. M. Čížek, J. Horáček, and W. Domcke, J. Phys. B **33**, L209 (2000).
[6] G. Knoth, M. Gote, M. Rädle, K. Jung, and H. Ehrhardt, Phys. Rev. Lett. **62**, 1735 (1989).
[7] J. P. Ziesel, I. Nenner, and G. J. Schulz, J. Chem. Phys. **63**, 1943 (1975).
[8] R. Abouaf and D. Teillet-Billy, J. Phys. B **10**, 2261 (1977).
[9] S. Živanov, M. Allan, M. Čížek, J. Horáček, F. A. U. Thiel, and H. Hotop, Phys. Rev. Lett. **89**, 073201 (2002).
[10] S. Živanov, M. Čížek, J. Horáček, and M. Allan, J. Phys. B **36**, 3513 (2003).
[11] J. Fedor, M. Cingel, J. D. Skalný, P. Scheier, T. D. Märk, M. Čížek, P. Kolorenč, and J. Horáček, Phys. Rev. A **75**, 022703 (2007).
[12] M. Allan and S. F. Wong, J. Chem. Phys. **74**, 1687 (1981).
[13] W. Domcke, Phys. Rep. **208**, 97 (1991).
[14] J. Horáček, M. Čížek, P. Kolorenč, and W. Domcke, Eur. Phys. J. D **35**, 255 (2005).
[15] M. Čížek, J. Horáček, A.-C. Sergenton, D. B. Popović, M. Allan, W. Domcke, T. Leininger, and F. X. Gadea, Phys. Rev. A **63**, 062710 (2001).
[16] I. S. Buchelnikova, Sov. Phys. JETP **35**, 783 (1959).
[17] L. G. Christophorou, R. N. Compton, and H. W. Dickson, J. Chem. Phys. **48**, 1949 (1968).
[18] R. Azria, L. Roussier, P. Paineau, and M. Tronc, Rev. Phys. Appl. **9**, 469 (1974).
[19] O. J. Orient and S. K. Srivastava, Phys. Rev. A **32**, 2678 (1985).
[20] D. Teillet-Billy and J. P. Gauyacq, J. Phys. B **17**, 4041 (1984).
[21] I. I. Fabrikant, S. A. Kalin, and A. K. Kazansky, J. Chem. Phys. **95**, 4966 (1991).
[22] M. A. Huels, J. A. Fedchak, R. L. Champion, L. D. Doverspike, J. P. Gauyacq, and D. Teillet-Billy, Phys. Rev. A **49**, 255 (1994).
[23] K. Aflatooni, A. M. Scheer, and P. D. Burrow, J. Chem. Phys. **125**, 054301 (2006).
[24] A. Modelli, J. Phys. Chem. A **109**, 6193 (2005).
[25] P. Rawat, V. S. Prabhudesai, G. Aravind, M. A. Rahman, and E. Krishnakumar, J. Phys. B **40**, 4625 (2007).
[26] M. Braun, M. W. Ruf, H. Hotop, P. Ciman, P. Scheier, T. D. Märk, E. Illenberger, R. P. Tuckett, and C. A. Mayhew, Int. J. Mass. Spectrom. **252**, 243 (2006).
[27] M. Allan, J. Electron Spectrosc. Relat. Phenom. **48**, 219 (1989).
[28] D. D. Briglia and D. Rapp, J. Chem. Phys. **42**, 3201 (1965).
[29] K. Aflatooni and P. D. Burrow, J. Chem. Phys. **113**, 1455 (2000).
[30] F. H. Read and N. J. Bowring, Charged particle optics program, CPO-3D, www.electronoptics.com
[31] D. Rapp and D. D. Briglia, J. Chem. Phys. **43**, 1480 (1965).
[32] D. Rapp and P. Englander-Golden, J. Chem. Phys. **43**, 1464 (1965).
[33] K. R. Asmis and M. Allan, J. Phys. B **30**, 1961 (1997).
[34] D. M. Pearl and P. D. Burrow, J. Chem. Phys. **101**, 2940 (1994).
[35] O. May, J. Fedor, B. C. Ibănescu, and M. Allan, Phys. Rev. A **77**, 040701(R) (2008).
[36] M. Allan, J. Phys. B **25**, 1559 (1992).
[37] R. Fandreyer, P. G. Burke, L. A. Morgan, and C. J. Gillant, J. Phys. B **26**, 3625 (1993).
[38] M. Čížek, J. Horáček, and W. Domcke, Phys. Rev. A **60**, 2873 (1999).
[39] W. Domcke and C. Mündel, J. Phys. B **18**, 4491 (1985).
[40] N. T. Padial and D. W. Norcross, Phys. Rev. A **29**, 1590 (1984).
[41] Y. L. Coat, R. Azria, and M. Tronc, J. Phys. B **15**, 1569 (1982).
[42] R. Azria, Y. L. Coat, D. Simon, and M. Tronc, J. Phys. B **13**, 1909 (1980).